Inverse Problems in Science and Engineering, Volume 13, Issue 2 April 2005 , pages 157 - 176

Parameter estimation in equivalent circuit analysis of dielectric cure monitoring signals using genetic algorithms

M.C. Kazilas, A.A. Skordos[1] and I.K. Partridge

Advanced Materials Department
School of Industrial and Manufacturing Science
Cranfield University, MK43 0AL, Cranfield, Beds, UK

This communication concerns the treatment of dielectric data obtained from experiments following the chemical hardening process (cure) in thermosetting resins. The aim is to follow, in real time, the evolution of the individual parameters of an equivalent electrical circuit that expresses the electrical behaviour of a curing thermoset. The paper presents a methodology for the sequential inversion of impedance spectra obtained in cure monitoring experiments. A new parameter estimation technique based on genetic algorithms is developed and tested using different objective functions. The influence of the objective functions on the modelling performance is investigated. The new technique models successfully spectra contaminated with high noise levels. The introduction of regularization in the optimisation function rationalises the effects of outliers usually detected in cure monitoring dielectric spectra. The technique was successfully applied to the analysis of series of spectra obtained during the cure of an epoxy thermosetting resin.

Keywords: Cure monitoring, equivalent circuit modelling, impedance, genetic algorithms, regularization

1. INTRODUCTION

Dielectric spectroscopy is an established experimental technique for probing molecular processes in polymers [1]. The use of the technique in studies of cure in thermosetting resins such as epoxies is also well established [2 – 7]. During the cure the thermosetting resin undergoes a transformation from a liquid to a rubber, as a result of the formation of a three dimensional molecular network, and then to a glass upon further advancement of the cross-linking reaction. In dielectric spectroscopy the electrical properties of the curing thermoset are measured over a wide frequency range as functions of time and of temperature. The spectra obtained give an insight into the material state at specific cure times, due to the strong dependence of the dielectric permittivity and dielectric loss, on the changing chemical and structural state of the material [1, 8]. Mijovic and co-workers have developed a slightly different but equivalent approach, based on the utilisation of the complex impedance spectrum [9 – 15]. The applicability of the technique to industrial process control is conditional on the existence of an efficient methodology for quantitative translation of the impedance spectra to material state.

In this paper, fitting of cure monitoring spectra is performed using genetic algorithms. Several objective functions are tested; namely weighted least squares, weighted absolute differences,

---

[1] *Current address: Centre for Micromechanics, Department of Engineering, University of Cambridge, Trumpington street, Cambridge, CB2 1PZ, United Kingdom*

least squares with logarithmic scaling of the experimental data and absolute differences with logarithmic scaling.

The effect of regularization on parameters estimation is also investigated. Simulated data with Gaussian noise and outliers are used for the assessment of the most appropriate objective function. Real experimental data are analyzed using the chosen objective function with and without the regularization term.

2. BASIC DIELECTRIC THEORY AND EQUIVALENT CIRCUIT MODELS

Three phenomena are present in the electrical response of a curing thermosetting resin at relatively low frequencies (1 Hz – 1 MHz): electrode polarisation, charge migration and dipolar relaxation [2, 10]. Consideration of these fundamental phenomena, backed up by experimental evidence, has led to the development of an equivalent circuit representation of the processes that affect the signal during the cure [9, 10]. The dipolar movements are modelled by a capacitor (C_{dip}) connected in series with a resistor (R_{dip}) and in parallel with another capacitor (C_{ind}). The first two elements represent the permanent dipoles, which are present in resins due to the charge distribution in asymmetric molecules or molecular groups [1], whilst the C_{ind} element represents the dipoles that are induced by the application of the electric field. A resistor (R_{ion}) models the presence of extrinsic and intrinsic charge carriers [2, 14, 15]. The resulting circuit is shown in Figure 1.

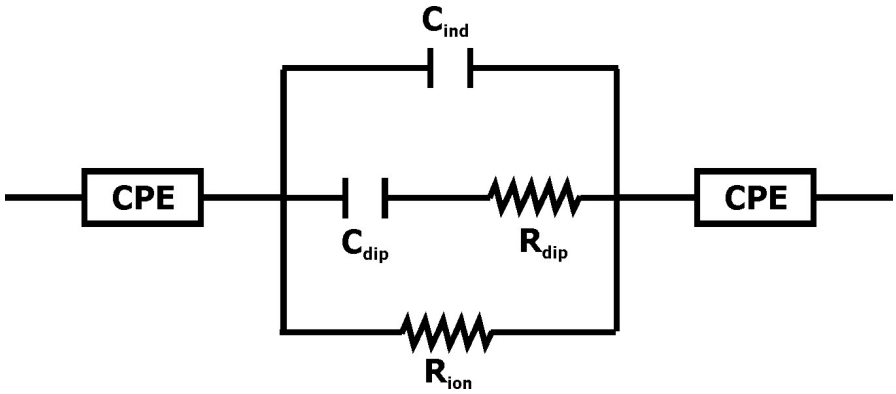

***Figure 1**: Equivalent circuit of epoxy thermoset*

Electrode polarisation, which originates from the accumulation of charges close to the surface of the embedded electrodes, is typically modelled using capacitors in series with the rest of the circuit [9, 10]. However, it has been reported that Constant Phase Elements model the non-ideal capacitive behaviour of the electrode-material interface more successfully [16]. The complex impedance Z_{CPE} of such an element is:

$$Z_{\mathrm{CPE}} = \frac{R_{\mathrm{el}}}{(j\omega)^n} \tag{1}$$

where ω is the angular frequency ($w = 2p f$) and R_{el}, n are the CPE parameters.
The complex impedance Z of the overall equivalent circuit, which is shown in Figure 1, is:

$$Z = Z' - jZ'' \tag{1}$$

where the real (Z') and imaginary (Z'') components are:

$$Z' = \frac{R_{ion}\left(\omega^2 C_{dip}^2 R_{dip}\left(R_{dip}+R_{ion}\right)+1\right)}{\omega^2\left(R_{ion}C_{dip}+R_{ion}C_{ind}+R_{dip}C_{dip}\right)^2+\left(\omega^2 R_{ion}C_{ind}R_{dip}C_{dip}-1\right)^2}+\frac{2R_{el}}{\omega^n}\cos\left(\frac{n\pi}{2}\right) \quad (2)$$

$$Z'' = \frac{\omega R_{ion}\left(\omega^2 R_{ion}C_{ind}R_{dip}^2C_{dip}^2+R_{ion}\left(C_{ind}+C_{dip}\right)\right)}{\omega^2\left(R_{ion}C_{dip}+R_{ion}C_{ind}+R_{dip}C_{dip}\right)^2+\left(\omega^2 R_{ion}C_{ind}R_{dip}C_{dip}-1\right)^2}+\frac{2R_{el}}{\omega^n}\sin\left(\frac{n\pi}{2}\right) \quad (3)$$

Relationships between the maximum of imaginary impedance and thermoset resistivity during cure have been established [10, 13]. The vitrification of the curing system has also been identified successfully using the impedance spectra [14]. However, fitting of the experimental data throughout the experimentally accessible frequency spectrum and determination of the evolution of circuit elements during the cure has not been attempted.

Equivalent circuit analysis is a general tool for data interpretation of complex systems [17]. Impedance spectra are usually fitted using weighted linear squares methods introduced by Macdonald [17 – 22]. The weight factors are a measure of the variance of each experimental point. As impedance is a complex variable, the real and imaginary components are fitted concurrently, taken as independent variables. Theoretically this is not true as the Kramers – Kronig transformation relates the real and imaginary part of such a variable [23, 24]. In practice, however, one needs to cover a very wide frequency spectrum for the transformation to give valid results [17].

The resulting objective function for the weighted linear squares has the following form:

$$S = \sum_{k=1}^{q}\left\{w_k'\left(Z'_{exp,k}-Z'_{mod,k}\right)^2+w_k''\left(Z''_{exp,k}-Z''_{mod,k}\right)^2\right\} \quad (4)$$

where S denotes the objective function, q is the number of measured frequencies and w_k are the weight factors for the real and imaginary parts of the complex impedance. The subscripts *exp* and *mod*, respectively, denote the experimental impedance value and that obtained from the application of equations 3 and 4.

Instead of the sum of squares, it is possible to use the sum of absolute differences as the objective function:

$$S = \sum_{k=1}^{q}\left\{w_k'\left|Z'_{exp,k}-Z'_{mod,k}\right|+w_k''\left|Z''_{exp,k}-Z''_{mod,k}\right|\right\} \quad (5)$$

The use of absolute differences is more robust than using the least squares method, in terms of tolerance to experimental outliers [25]. In cure monitoring the impedance values change several orders of magnitude (typically 10^3 – 10^9 Ohm) during the experiment and towards the end of cure they reach the limit of the apparatus measuring range. For the apparatus used in this study – and for most of the commercially available instruments – this means that measurement scatter can be as high as 10%. Furthermore, interference with other electrical equipment is possible, resulting in spurious outliers. Dygas and Breiter have proposed a method for detecting and eliminating outliers in impedance spectra by comparing each experimental point with its estimated standard deviation [26]. However, this method is not suitable for analyzing consecutive spectra, as it demands replicate scans for the calculation of standard deviation. In a cure monitoring experiment, the impedance spectrum changes as the cure progresses and it is not possible to repeat the measurement as the state of the material changes irreversibly.

One way to enhance the robustness of the objective function is to add a regularization term [27]. For the case of absolute differences, we have:

$$S = \sum_{k=1}^{q} \left\{ w'_k \left| Z'_{\exp,k} - Z'_{\mathrm{mod},k} \right| + w''_k \left| Z''_{\exp,k} - Z''_{\mathrm{mod},k} \right| \right\} + \lambda \sum_{k=1}^{P_{\mathrm{no}}} \left\{ w_k^{\mathrm{par}} \left| \mathrm{par}_k - \mathrm{par}_{k,\exp} \right| \right\} \quad (6)$$

where λ is the Tikhonov regularization parameter [27], P_{no} is the number of fitting parameters (the number of circuit elements in Figure 1), par_k are the parameter values and $par_{k,exp}$ is an estimation of the expected parameter values. A similar expression can be obtained for the least squares case.

The presence of the regularization term suppresses any irregular fluctuations imposed by large errors or outliers on the estimated parameters [27]. Winterhalter and co-workers have used an objective function with a Tikhonov regularization term to model admittance spectra [28, 29]. They fitted a continuous distribution of relaxation functions to experimental data and argued that without the regularization term the number of significant relaxation peaks had to be chosen arbitrarily before any fitting was performed.

The fitting is performed by minimizing the objective function. Macdonald has developed a software code [30] for solving the minimisation problem in the case of impedance spectra, based on the Levenberg – Marquardt method [31]. The success of the minimisation depends strongly on the initial estimates of the sought parameters. Furthermore, there is always a possibility of the algorithm converging to a local instead of the global minimum.

In contrast to hill-climbing methods, genetic algorithms provide global minimisation and fitting capabilities especially in the case of multivariate systems [32]. VanderNoot and Abrahams have utilised genetic algorithms to fit impedance spectra [33], using an objective function based on weighted absolute differences. Yang and co–workers have also implemented genetic algorithms to model admittance data [34], with a weighted least squares objective function.

3. ARTIFICIAL IMPEDANCE SPECTRA AND GENETIC ALGORITHM

Construction of simulated spectra

The values of the circuit parameters used to generate artificial spectra are given in Table I. They are representative of epoxy resin response in the early stages of cure, when the resin is liquid. The resulting spectra are shown in Figure 2.

It can be observed that the real impedance values are nearly constant at low frequencies and decrease rapidly at higher frequencies. (The slight drop observed in the very low frequency region is a consequence of electrode polarisation.). The imaginary impedance spectrum exhibits a minimum and a maximum, with the peak value relating to the extent of the charge migration in the system.

Table I: *Circuit element values for the construction of simulated spectra*

R_{ion} (Ohm)	R_{dip} (Ohm)	C_{dip} (F)	C_{ind} (F)	R_{el} (Ohm)	n
10^6	10^4	2×10^{-12}	10^{-11}	10^6	0.5

The sensitivity of the resulting real and imaginary impedance spectra to the circuit parameters was investigated. Each of the circuit parameter value was altered by ± 10% whilst all the other parameters were kept constant. The average percentage difference from the original spectrum

was used as a measure of sensitivity over the whole frequency region. The results are summarized in Table II.

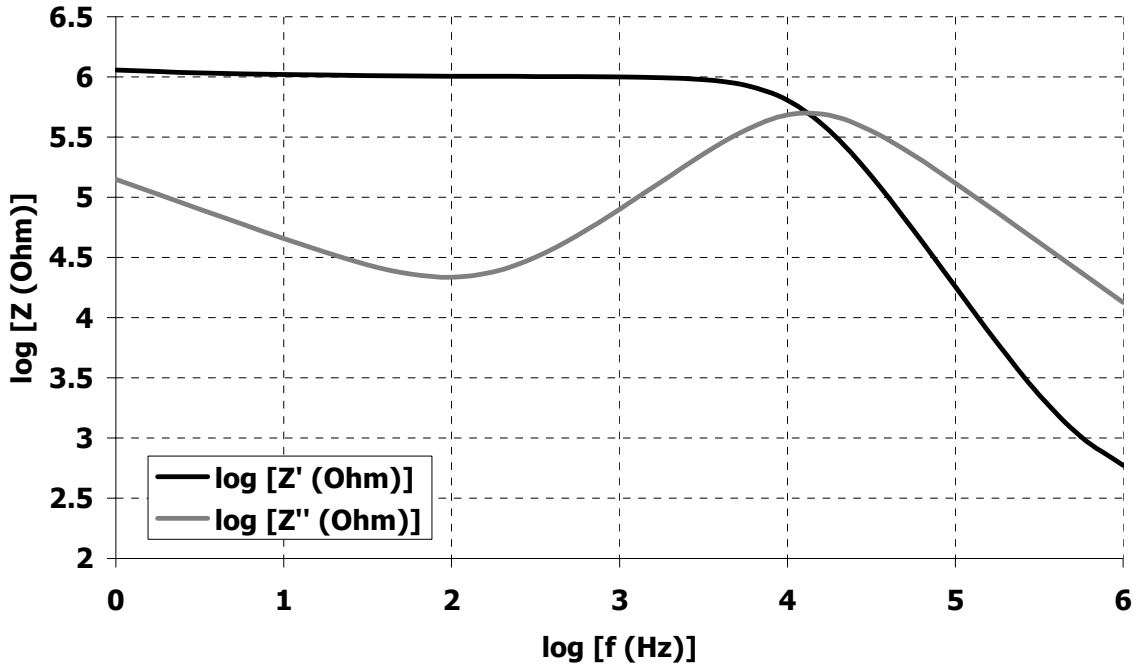

Figure 2: *Real and Imaginary impedance spectra typical of a particular given state in epoxy resin cure. The equivalent circuit used is shown in Figure 1 and the circuit element values are given in Table I.*

It can be observed that the spectra are sensitive to changes in R_{ion} and C_{ind}, whilst the influence of R_{dip} and C_{dip} is less marked. It should be noted that the sensitivity of the impedance to each circuit parameter depends on the frequency. Electrode polarisation parameters, for example, have greater impact on the signal at low frequencies.

Table II: *Sensitivity to circuit parameters expressed as the average percentage difference from the original case for a ± 10% change in the parameter*

		R_{ion} (Ohm)	R_{dip} (Ohm)	C_{dip} (F)	C_{ind} (F)	R_{el} (Ohm)	n
Z'	**+ 10%**	8.42	0.58	1.34	6.14	0.25	2.21
	- 10%	7.10	0.01	1.03	5.36	2.86	2.61
Z''	**+ 10%**	8.00	0.57	1.35	4.95	0.25	1.12
	- 10%	7.56	0.01	1.02	4.96	2.86	2.52

A noise signal with a Gaussian distribution was added to the simulated values in order to assess the robustness of the estimation algorithm. The error values were taken by sampling the normal distribution with mean 1 and standard deviation 0.033. These values were then multiplied with the simulated values. The final simulated spectra contained a 10% maximum error.

Genetic algorithm

The flow chart of the binary genetic algorithm used for the minimisation is illustrated in Figure 3. The main parameters of the algorithm are the number N of solution vectors per

generation (individuals), the maximum number of generations G_{max}, the exchange probability p_e and the mutation probability p_m. The solution vectors are sorted and a predefined number (N_e) of the fittest individuals is passed to the next generation (elitism). Then, the solution vectors are encoded in binary format (each parameter in the vector becomes a sequence of 100 genes) and the crossover and mutation operations are applied.

The crossover operation is performed by selecting two encoded individuals and exchanging their bits. The selection of the individuals is proportional to their fitness (fitter individuals are more likely to be selected). The bits to be exchanged are selected with probability p_e. If this probability is met the bits of the two individuals are exchanged ($0 \leftrightarrow 1$). The crossover operation produces two new offspring per iteration. Therefore, the number of iterations for the formation of a new generation of solutions will be:

$$\text{Number of iterations for generation of new offspring} = \frac{N - N_e}{2} \tag{7}$$

In the coding of the algorithm, iteration i produced the offspring i and $i+1$. For this reason the number of individuals N (and N_e) is an odd number.

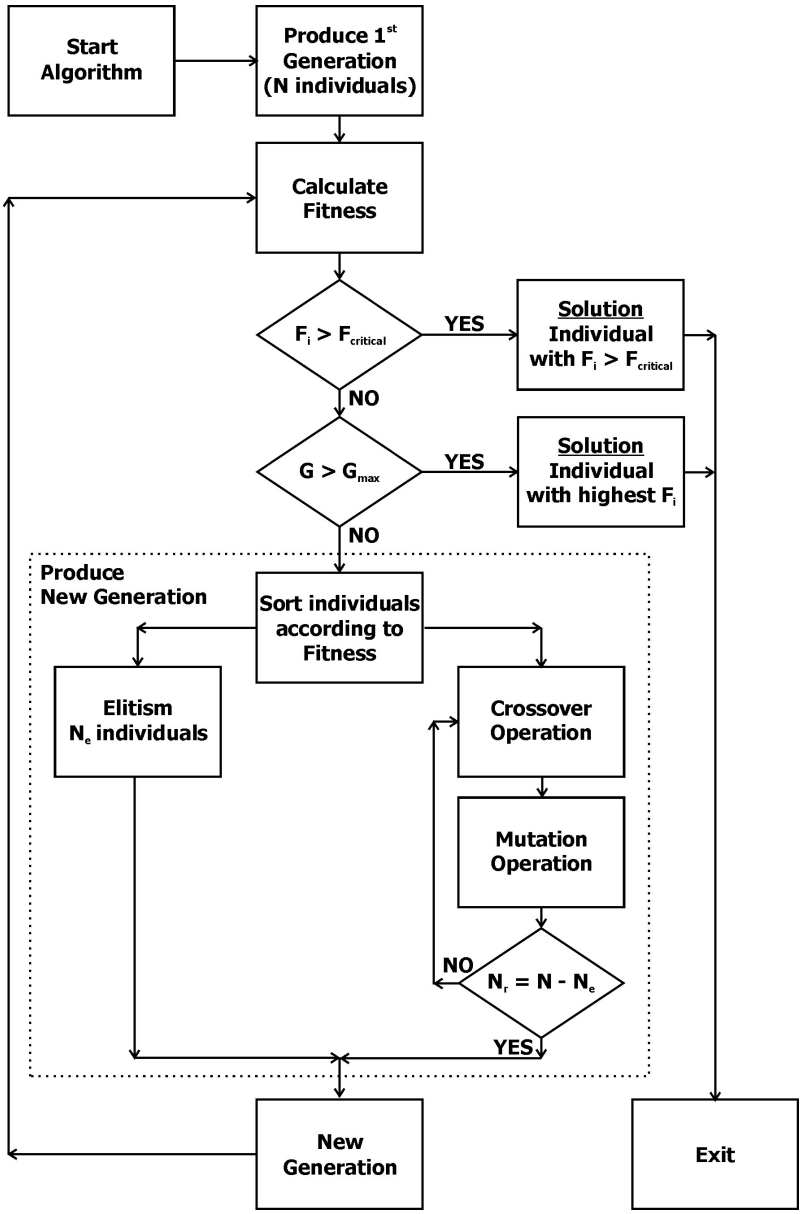

Figure 3: *Genetic algorithm flowchart*

The mutation operation is performed by selecting a bit of an individual with probability p_m and changing that bit from zero to one or vice versa. The probability p_m changes for each successive generation according to the dispersion of the solution vectors (adaptive mutation):

$$p_{\mathrm{m}} = \frac{1}{2}\exp\left(-c\sqrt{\frac{\text{Fitness deviation}}{\text{Average fitness}}}\right) \tag{8}$$

where c is a parameter that determines the range of values of p_m (choice of high c leads to lower values of p_m). For this application $c = 6$. If the resulting p_m was below 0.001, which means that the fitness deviation is very low (candidate solution values are very close), the mutation probability was reset to 0.025 to ensure further exploration of the solution search space.

The crossover operation explores the candidate solution vector space and builds new, fitter, solutions. The mutation operation ensures that the whole solution space is explored.

The fitness function F used can be expressed as follows:

$$F = \frac{100}{S_i + 1} \quad i = 1, 2, 3 \text{ or } 4 \tag{9}$$

where S_i is the selected objective function. A list of all the objective functions used in this investigation is given in Table III.

Table III: *Objective functions tested without any regularization term*

S_1	Weighted least squares	$S = \sum_{k=1}^{q} \left\{ \left(\frac{Z'_{\exp,k} - Z'_{\mathrm{mod},k}}{Z'_{\mathrm{mod},k}} \right)^2 + \left(\frac{Z''_{\exp,k} - Z''_{\mathrm{mod},k}}{Z''_{\mathrm{mod},k}} \right)^2 \right\}$
S_2	Weighted absolute differences	$S = \sum_{k=1}^{q} \left\{ \left\| \frac{Z'_{\exp,k} - Z'_{\mathrm{mod},k}}{Z'_{\mathrm{mod},k}} \right\| + \left\| \frac{Z''_{\exp,k} - Z''_{\mathrm{mod},k}}{Z''_{\mathrm{mod},k}} \right\| \right\}$
S_3	Logarithmic scaling – least squares	$S = \sum_{k=1}^{q} \left\{ \left[\log(Z'_{\exp,k}) - \log(Z'_{\mathrm{mod},k}) \right]^2 + \left[\log(Z''_{\exp,k}) - \log(Z''_{\mathrm{mod},k}) \right]^2 \right\}$
S_4	Logarithmic scaling – absolute differences	$S = \sum_{k=1}^{q} \left\{ \left\| \log(Z'_{\exp,k}) - \log(Z'_{\mathrm{mod},k}) \right\| + \left\| \log(Z''_{\exp,k}) - \log(Z''_{\mathrm{mod},k}) \right\| \right\}$

The fitness function varies from zero ($S_i \rightarrow \infty$) to 100 ($S_i \rightarrow 0$). The algorithm terminates when an individual with fitness higher than a predefined value ($F_{critical}$) is found or when G_{max} is reached.

Test runs of the genetic algorithm were performed using the spectra of Figure 2 . The search space for each parameter is given in Table IV. Parameters with greater sensitivity were given a smaller space to explore.

Weighted least squares were used as the objective function in these test runs. The fitness value of the final solution was used for comparing the different scenarios. For a number of generations G_{max}, the best obtained fitness was divided by a final fitness value which was attained after 200 generations. For each scenario the algorithm ran 10 times. The average values of the results of each of the runs are reported in Table V.

Table IV: *Search space of the fitting parameters*

	R_{ion} (Ohm)	R_{dip} (Ohm)	C_{dip} (F)	C_{ind} (F)	R_{el} (Ohm)	n
Upper limit	1.25×10^{6}	4.95×10^{4}	1.90×10^{-12}	1.25×10^{-12}	1.95×10^{6}	0.625
Low limit	7.50×10^{5}	5.00×10^{2}	1.00×10^{-13}	7.50×10^{-13}	5.00×10^{4}	0.375
Space size	5.00×10^{5}	4.90×10^{4}	1.80×10^{-12}	5.00×10^{-13}	1.90×10^{6}	0.250

Table V: *Fitting results for the tuning of the genetic algorithm parameters*

Exchange probability value (p_e)	**Maximum Fitness value**	**Standard Deviation**

0.4	95.41	4.242
0.5	95.12	4.052
0.6	94.25	3.351
Number of generations (G_{max})	**Fitness value divided by the maximum fitness**	**Standard deviation**
60	0.996	2.45×10^{-3}
80	0.998	1.22×10^{-3}
100	1.000	0.51×10^{-3}
120	1.000	0.05×10^{-3}
140	1.000	0.02×10^{-3}
Number of individuals (N)	**Maximum Fitness value**	**Standard deviation**
81	95.32	4.700
101	94.50	4.785
121	94.48	4.126

It can be observed that p_e values in the range of 0.4 – 0.6 do not affect the algorithm performance. The maximum fitness value is obtained when the number of generations G_{max} is close to 100. Higher G_{max} values make the algorithm slower, without improving its performance. The population number N does not affect the algorithm performance when its value is higher than 81. The final algorithm parameter values are given in Table VI.
Each of the fittings reported in the Results section below was repeated 50 times except for the fitting of experimental data. The average fitness values from the 50 runs are presented. The errors of the estimated values are calculated assuming Gaussian distribution and 95% level of confidence.

Table VI: *Final values for the genetic algorithm implementation*

Maximum number of generations (G_{max})	**Number of solution vectors (individuals) (N)**	**Elitism (N_e)**	**Exchange Probability (p_e)**	**Initial Mutation Probability (p_m)**
100	101	9	0.5	0.025

4. RESULTS

Determination of the optimum objective function

The results from the runs for the different objective functions (listed in Table III) are given in Table VII and are to be compared with the true values, shown in Table I.

Table VII: *Results from test runs on noisy data for the determination of the objective function*

	R_{ion} (Ohm)	**R_{dip} (Ohm)**	**C_{dip} (F)**	**C_{ind} (F)**	**R_{el} (Ohm)**	**n**
S_1	1000391	23793	$1.35\text{x}10^{-12}$	$1.02\text{x}10^{-11}$	1010811	0.503
S_2	1003824	14534	$1.68\text{x}10^{-12}$	$1.02\text{x}10^{-11}$	1015095	0.505
S_3	1004254	16695	$1.59\text{x}10^{-12}$	$1.03\text{x}10^{-11}$	1017422	0.506
S_4	1005266	15424	$1.67\text{x}10^{-12}$	$1.02\text{x}10^{-11}$	1019466	0.507

	% Percentage difference compared to the true values					
S_1	0.04	137.93	32.55	2.28	1.08	0.69
S_2	0.38	45.34	15.94	2.23	1.51	0.90
S_3	0.43	66.95	20.69	2.78	1.74	1.13
S_4	0.53	54.24	16.00	2.10	1.95	1.41
	Standard deviation (normalised by the corresponding means)					
S_1	$1.25\text{x}10^{-3}$	$1.67\text{x}10^{-1}$	$6.80\text{x}10^{-2}$	$8.02\text{x}10^{-3}$	$9.11\text{x}10^{-3}$	$7.95\text{x}10^{-3}$
S_2	$1.03\text{x}10^{-3}$	$1.10\text{x}10^{-1}$	$5.83\text{x}10^{-2}$	$8.17\text{x}10^{-3}$	$5.93\text{x}10^{-3}$	$5.94\text{x}10^{-3}$
S_3	$1.82\text{x}10^{-3}$	$1.24\text{x}10^{-1}$	$6.48\text{x}10^{-2}$	$7.39\text{x}10^{-3}$	$9.22\text{x}10^{-3}$	$5.93\text{x}10^{-3}$
S_4	$1.28\text{x}10^{-3}$	$1.38\text{x}10^{-1}$	$5.78\text{x}10^{-2}$	$7.96\text{x}10^{-3}$	$9.21\text{x}10^{-3}$	$5.92\text{x}10^{-3}$

Table VII indicates the estimation accuracy for each of the circuit parameters. Values of R_{ion}, C_{ind}, R_{el} and n exhibit errors below 3%, for all the objective functions tested, whilst R_{dip} and C_{dip} exhibit significant errors. From the percentage errors it is apparent that the weighted least squares objective function (S_1) results in the most accurate R_{ion}, C_{ind}, R_{el} and n values, however, the estimates of R_{dip} and C_{dip} are poor.

The rest of the objective functions give similar results. The accuracy of the R_{ion}, C_{ind}, R_{el} and n values estimations is close to the results obtained using S_1. The estimations of R_{dip} and C_{dip} are much better than those obtained with S_1, especially in the case of the absolute differences objective functions (S_2 and S_4). The logarithmic scaling objective functions give similar estimations compared to the objective functions using weight factors.

Effect of the regularization parameter on spectra containing outliers

Spectra containing 10% Gaussian error and four outlier points were fitted using the S_4 objective function with a regularization term as follows:

$$S_5 = \sum_{k=1}^{25} \left\{ \left| \log\left(Z'_{\exp,k}\right) - \log\left(Z'_{\mathrm{mod},k}\right) \right| + \left| \log\left(Z''_{\exp,k}\right) - \log\left(Z''_{\mathrm{mod},k}\right) \right| \right\} + \lambda \sum_{k=1}^{6} \left\{ \frac{\left|\mathrm{par}_k - \mathrm{par}_{k,\exp}\right|}{\mathrm{par}_{k,\exp}} \right\} \tag{10}$$

The fitted spectrum is illustrated in Figure 4.

Three outliers were placed in the frequency area close to 60 Hz. This frequency region is more vulnerable to noise coming from external electric devices. The last outlier was placed at 1 Hz. The expected values par_{exp} are given in Table I.

The dependence of the estimated circuit parameters on the regularization parameter value λ is shown in Figure 5. The initial value ($\lambda=0$) means that the fitting is performed without the regularization term.

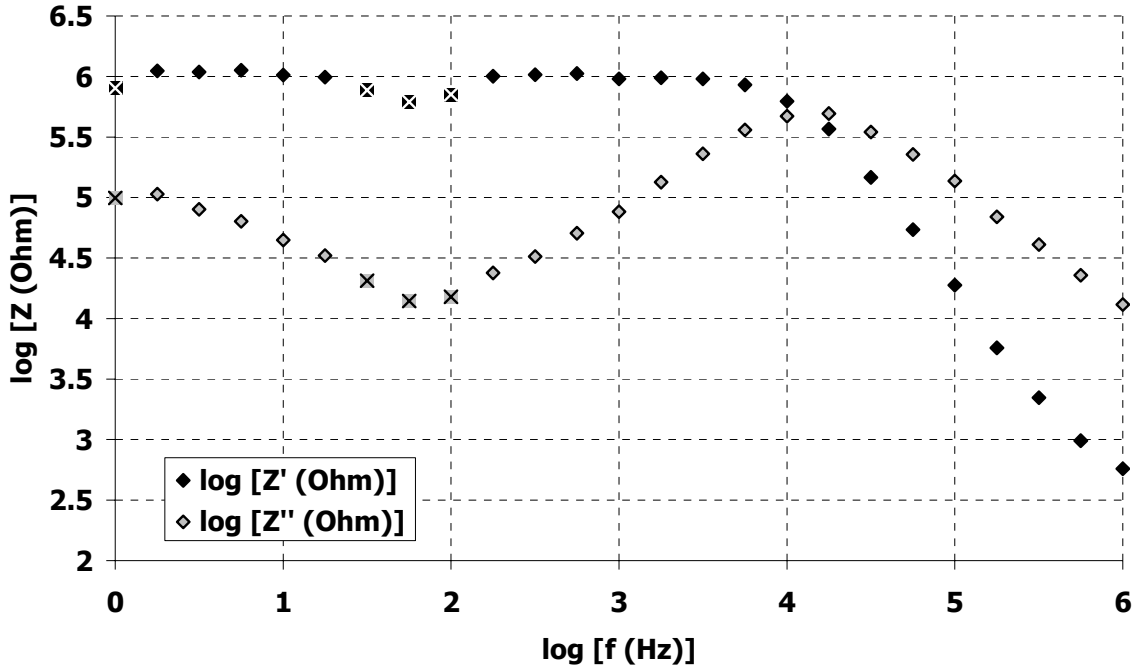

Figure 4: *Impedance spectrum with 4 outliers (indicated by crosses at log[f(Hz)] = 0, 1.5, 1.75 and 2) and 10% random Gaussian noise*

It is observed that the charge carriers resistance R_{ion} estimation does not depend on the regularization parameter. The estimated value has a 2% error compared to the true value. The dipolar resistance R_{dip} estimation shows some dependence on the regularization term. Without the regularization term – or with $\lambda < 0.2$ – there is a 20% error on the estimation. As the regularization parameter increases the estimation error is reduced. This improvement of the estimation becomes less significant for $\lambda > 1$. Similar behaviour is observed in the estimation of C_{dip}. The initial estimation error of approximately 8% is reduced to less than 2% when $\lambda \geq 1$. The induced capacitance C_{ind} estimation is very good –less than 3% error- with or without the regularization term. A further improvement, however, is observed for λ close to unity. The electrode polarization parameters have a more significant dependence on λ. R_{el} has an error of about 8% without regularization, which is reduced to less than 1% when $\lambda = 1$ and stays low for higher λ values. The estimation error in the exponent n is over 15% without regularization, which is reduced to approximately 5% when $\lambda > 1$.

Experimental cure monitoring data and modelling

Experimental results

Having established the principle of use of the genetic algorithm in modelling of artificial spectra, the approach was implemented and tested on a set of real cure monitoring data. The material used for the acquisition of the experimental data set was RTM6, an aerospace grade epoxy resin supplied by Hexcel® Composites UK. The resin was cured isothermally at 150°C. A Solartron Analytical® 1260 Gain – Phase Analyzer was used to obtain the impedance data over the frequency range from 1Hz to 1MHz. A total of 25 frequencies were measured. The duration of each frequency sweep was ~2min. Temperature control to within 0.1°C was achieved through a 2408 Eurotherm® temperature controller. The dielectric sensor used has a typical comb-electrode geometry and is commercially available from Pearson Panke Ltd (GIA sensor) – see Figure 6.

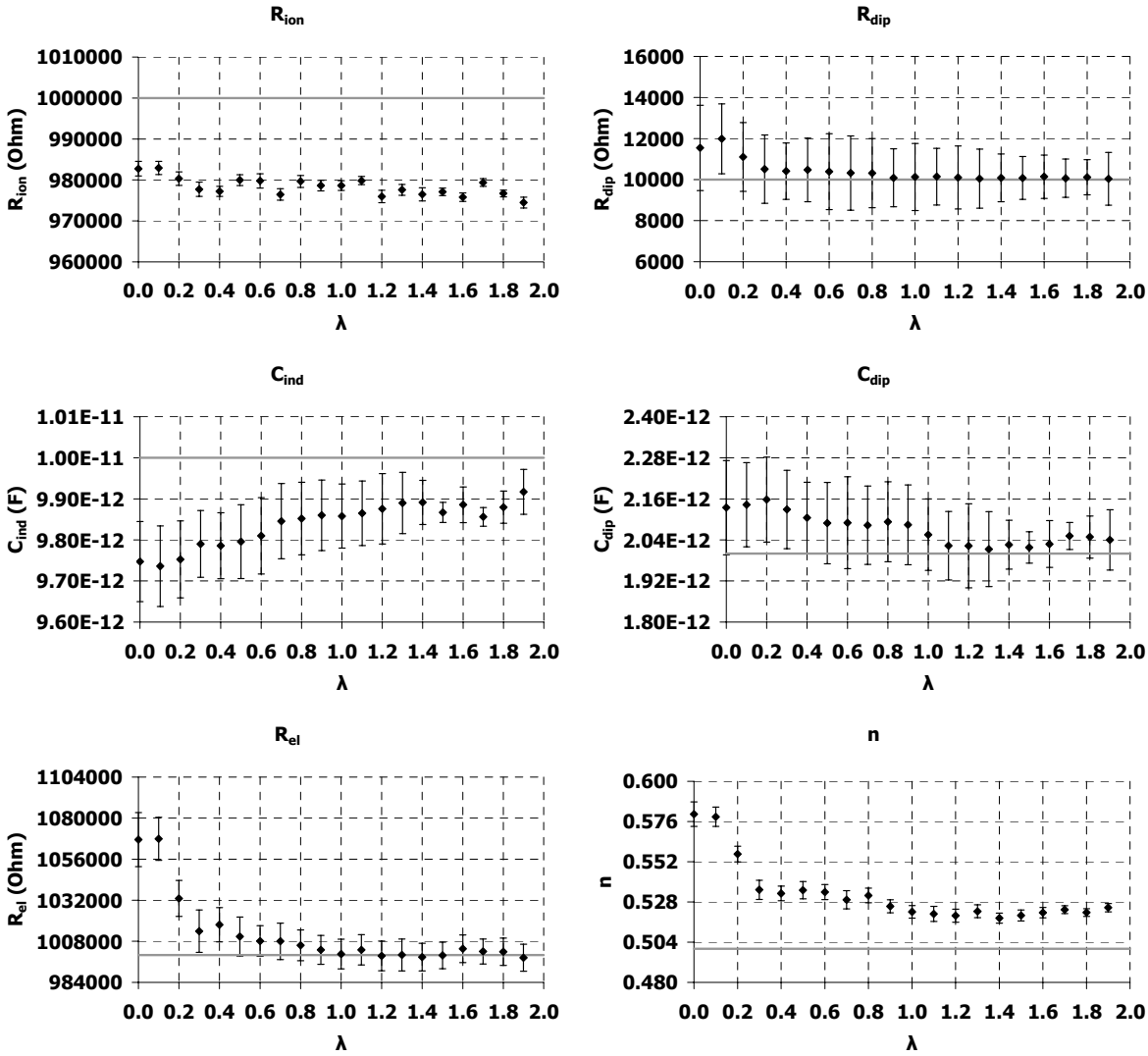

Figure 5: *Dependence of circuit parameters on the regularization parameter. The fitted spectrum is shown in Figure 4. The correct values are denoted by the grey line.*

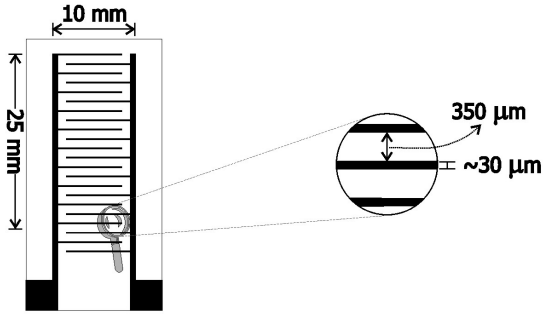

Figure 6: *Geometry of GIA dielectric sensor*

Impedance spectra from the cure of RTM6 are shown in Figures 7 and 8. The signal is dominated by charge carriers [10]. In both figures, the shift of both the real and imaginary impedance towards higher values and lower frequencies as the cure progresses is observed. The experimental points below Z' equal to 1kOhms, on the high frequency side of the real impedance spectrum, are considered to be of limited validity (possible outliers).

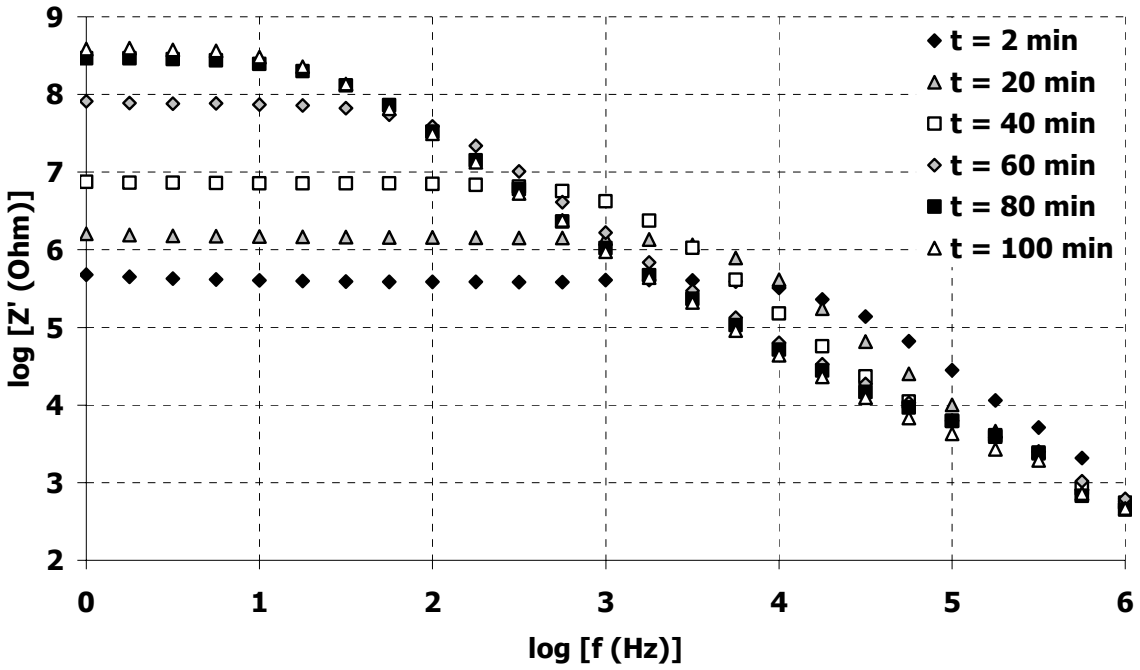

Figure 7: *Real impedance spectrum evolution for the isothermal cure of RTM6 at 150°C*

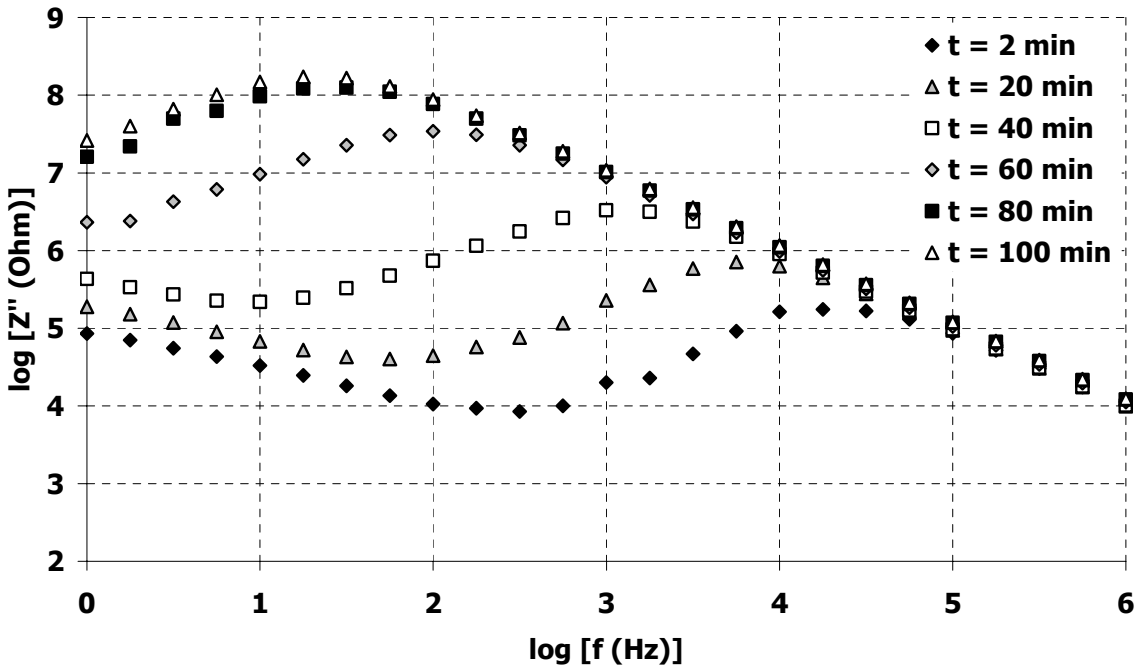

Figure 8: *Imaginary impedance spectrum evolution for the isothermal cure of RTM6 at 150°C*

Initially the material is in the liquid phase and no reaction has taken place. This means that the impedance values are relatively low. As the polymerisation reaction proceeds, the average molecular weight of the polymer chains increases and a three – dimensional network starts to form. This network formation impedes the movements of charge carriers and results in higher impedance values. Towards the end of the cure, the resin vitrifies. Charge carriers movements are strongly hindered in the final glassy state of the polymer. Impedance spectra settle at very

high final values and any further increase with time is negligible. Electrode polarisation is dominant at low frequencies in the imaginary impedance spectrum. As the cure progresses, this region moves out of the experimental frequency range.

Application of genetic algorithm

The first two spectra, corresponding to 2 min and 4 min (not shown in Figures 7 and 8) respectively, were fitted without the regularization term. The fitted parameters were then used for the calculation of the par_{exp} estimates, for the fitting of the next spectrum. Linear extrapolation was used as follows:

$$\mathrm{par}_{k,\exp}^{t_3} = \frac{\mathrm{par}_{k,\exp}^{t_2}(t_3 - t_1) - \mathrm{par}_{k,\exp}^{t_1}(t_3 - t_2)}{t_2 - t_1} \xrightarrow{\substack{\text{constant} \\ \text{time step}}} \mathrm{par}_{k,\exp}^{t_3} = 2\mathrm{par}_{k,\exp}^{t_2} - \mathrm{par}_{k,\exp}^{t_1} \quad (11)$$

where the exponents t_i, $i = 1,2,3$ denote the average time where the impedance spectrum data were recorded. For every frequency sweep, t_i is given by:

$$t_i = \frac{1}{2}([\text{time of 1st measurement}] - [\text{time of last measurement}]) \quad (12)$$

The effect of the regularization term is that it penalises irrational jumps in the circuit parameter values. The physical meaning of such a constraint is that the equivalent circuit elements are expected to evolve gradually during the cure. For the estimation of the consecutive spectra the objective function of equation (9) was used. The search space was adjusted for each spectrum according to the parameter values obtained on the preceding spectrum. These parameter values were set as the mean of the corresponding search range for the new spectrum. Table VIII shows the ranges for all the circuit parameters. If any of the newly estimated parameters were within 1% of the limits of the search space, the search space of all the parameters was expanded by 10% and the genetic algorithm was rerun. A schematic of the whole modelling methodology is shown in Figure 9.

Table VIII: *Adaptive search space of the fitting parameters. Subscript p denotes the parameter values obtained from fitting the chronologically preceding spectrum.*

	$R_{ion,\,new}$ (Ohm)	$R_{dip,\,new}$ (Ohm)	$C_{dip,\,new}$ (F)	$C_{ind,\,new}$ (F)	$R_{el,\,new}$ (Ohm)	n_{new}
Mean	$1.00\times R_{ion,p}$	$5.05\times R_{dip,p}$	$5.05\times C_{dip,p}$	$1.00\times C_{ind,p}$	$1.25\times R_{el,p}$	$1.00\times n_p$
Range	$0.99\times R_{ion,p}$	$4.95\times R_{dip,p}$	$4.95\times C_{dip,p}$	$0.25\times C_{ind,p}$	$0.75\times R_{el,p}$	$0.25\times n_p$

Two runs were performed: one without the regularization term and one with the regularization term with $\lambda = 1$. The fitting results with and without regularization are illustrated in Figure 10. The charge migration resistance estimation, which is the parameter with respect to which the impedance data have the greatest sensitivity, is not affected by the regularization. R_{ion} values change several orders of magnitude during the cure. Similarly to R_{ion}, C_{ind} values are not affected by regularization. The dipolar resistance R_{dip} is very noisy when the fitting is performed without regularization. The introduction of regularization reduces the noise significantly. The same is observed for C_{dip}. The electrode polarization parameters are more influenced by the existence of the regularization term. Fitting without regularization leads to very large values of R_{el}. The exponent n values have a percentage difference that exceeds 40% in the later stages of the cure.

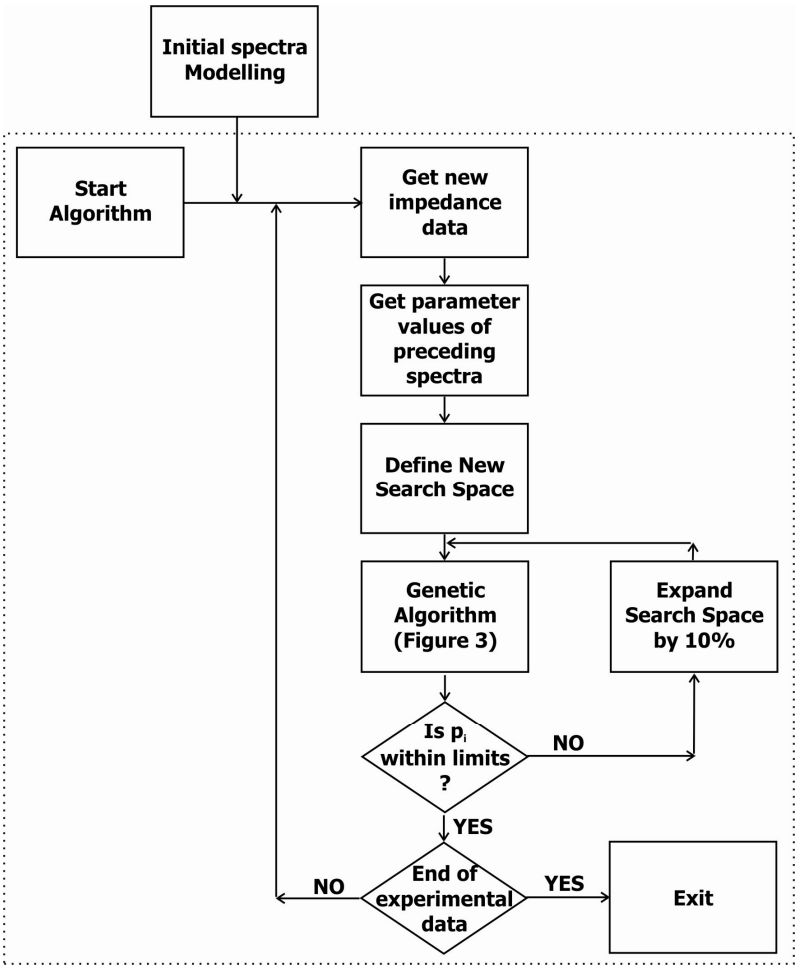

Figure 9: *Methodology for modelling consecutive spectra*

6. DISCUSSION

Choice of suitable objective function

The simulation results have shown that there are minor differences between an objective function based on least squares and one based on absolute differences. The use of least squares tends to give slightly better estimations of the more sensitive parameters such as R_{ion}. In contrast, when a least squares objective function is used, the estimation of the least sensitive parameters leads to erroneous results (for example, see R_{dip} and C_{dip} estimations in Table VII). The use of absolute differences gives better approximations to parameters with lower sensitivities such as R_{dip} but compromises accuracy of the estimation of parameters with respect to which the model circuit shows high sensitivity. In the case of cure monitoring spectra, the determination of parameters with low sensitivity is important, as they contain information about the dipolar movements of the curing system [9, 10]. Dipolar movements are directly linked to the vitrification of thermosets [2], a very important milestone in the cure process. Therefore the use of absolute differences is considered more beneficial. The use of logarithmic scaling instead of weighted residuals did not improve or worsen the simulation. Logarithmic scaling has the advantage that no estimation of the experimental data variance is needed as input to the objective function, as is the case when weight factors are used.

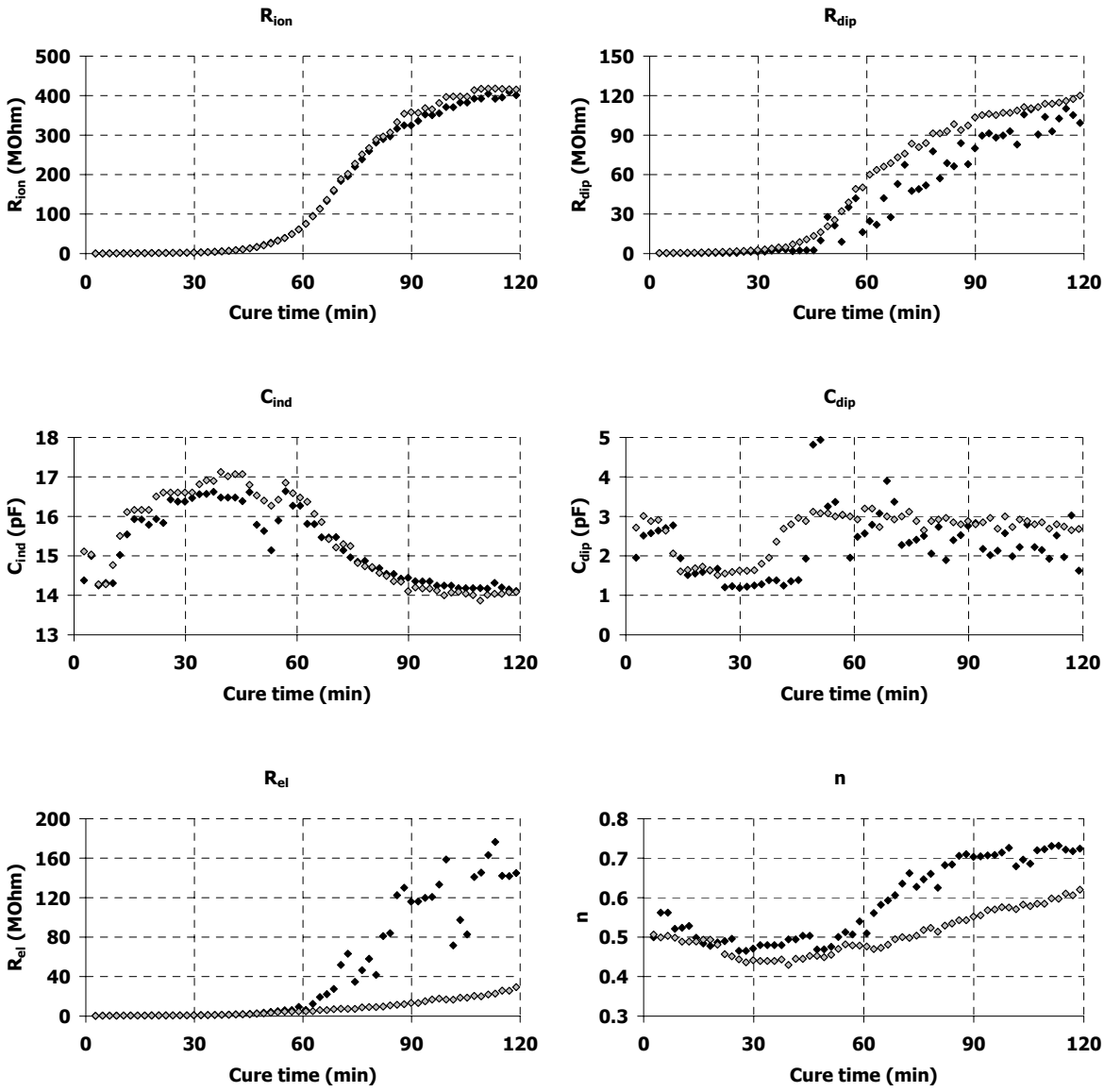

Figure 10: *Equivalent circuit parameters for the isothermal cure of RTM6 at 150 °C. Black points show the fitting without regularization. Grey points show the fitting when the regularization term is added to the objective function.*

Effect of regularization

From Figure 5 it is evident that regularization helps in reducing the effect of outliers in the estimation. This is more pronounced in the electrode polarization circuit parameters R_{el} and n. The outliers, as shown in Figure 4, are placed in the low frequency side of the spectrum, as sources of noise are much more likely to affect this frequency region. Consequently, the presence of outliers is expected to affect electrode polarisation more severely, as the electrode polarisation term dominates the response of the curing system at low frequencies (see equations (2)-(3)) [3, 16].

The presence of outliers is always a danger in cure monitoring signals, especially at frequencies close to 60 Hz. Minimisation of the detrimental effects of outliers on curve fitting is extremely helpful in cases where the identification and elimination of outliers is not feasible. One of the aims in analysing cure monitoring spectra is to automatically model consecutive spectra and to use the circuit parameter values for characterising the cure. The enhanced robustness that the regularization offers is a step further towards this aim.

Fitting of consecutive cure monitoring spectra

The fitting of consecutive experimental spectra showed the potential of regularization in dealing with real cure experiment data. The spectrum moves continuously and slowly during the cure. It is therefore expected that the circuit parameter values will change accordingly. This is crucial for the regularization to work, as the expected parameter values are obtained from the fitting of the chronologically preceding spectra. In the experiment studied, the curing process takes over 100 minutes to complete (in industrial processes it can be several hours), whilst the data acquisition process for the whole spectrum takes about 2 min. This implies that the value changes between two consecutive impedance spectra are in the order of 2% of the total difference between the start and the end of the experiment.

In the estimation of R_{ion} and C_{ind} the use of regularization does not influence the quality of the estimated values. The trend is the same with the estimates obtained without regularization. This is a result of the very high sensitivity of the spectra to R_{ion} and C_{ind}. Small changes in those parameters can lead to large estimation errors. It is therefore expected that their values are estimated accurately with or without regularization. In the estimation of R_{dip} and C_{dip} smoother data are obtained with regularization. The trend in R_{dip} is more clearly seen and a step increase in C_{dip} can be resolved. The R_{dip} and C_{dip} values are less influential in the overall signal. The use of regularization forces the genetic algorithm to explore values close to the mean (see Table VIII) without losing the ability of exploiting the whole solution search space.

The dipolar movements in thermosetting systems are connected with the cure induced vitrification [35, 36] and the product of R_{dip} and C_{dip} gives a measure of the dipolar relaxation time τ_{dip} [9]. In commercial systems the presence of charge carriers obscures the effect of the dipoles on the signal. The proposed parameter estimation technique is able to uncover and model adequately the dipolar movements in such systems and thus offers an efficient way for identifying vitrification in situ.

The big discrepancy in the electrode polarization circuit elements estimation can be attributed to the movement of the spectrum during the cure. The spectrum initially contains a frequency region where electrode polarization dominates the signal. This region lies at low frequencies and can be identified easily in the imaginary impedance spectrum. As the spectrum moves to the left, this region moves out of the frequency range of the experiment (e.g. in Figure 8, the minimum point cannot be seen for $t > 60$ min). This means that the sensitivity with respect to R_{el} and n is reduced and erroneous values are obtained from the parameter estimation. Regularization forces the estimated values not to vary much from the values obtained in the previous fit. This prevents parameters with low sensitivity from settling to abnormal values and thus affecting the estimation of other parameters.

7. CONCLUSIONS

Genetic algorithms were used in order to estimate the values of the parameters of an equivalent circuit expressing the dielectric behaviour of thermosetting polymers during cure. The parameters change by several orders of magnitude in value during the reaction, whilst the existence of noise and outliers makes the inversion a challenging problem.

Several objective functions based on least squares and absolute differences for the minimisation problem were tested. Absolute differences were found to be more accurate in modelling cure monitoring spectra, due to their higher accuracy in estimating parameters of low sensitivity. Logarithmic scaling of the experimental data worked equally well with weighting.

The robustness of absolute differences was enhanced with the incorporation of a regularization term in the objective function. Regularization lends itself to the inversion

problem at hand, as the parameter values of consecutive spectra are expected to have close values. As a result regularization using the previous solution reduces the effect of outliers and noise in the modelling of experimental spectra. This enables efficient use to be made of the estimation algorithm in real time analysis of cure monitoring spectra.
The technique presented here can discern the contribution of permanent dipoles in the impedance spectrum of commercial thermosetting systems where charge carriers usually dominate the signal. This constitutes a significant improvement in dielectric cure monitoring analysis as it overcomes the difficulties faced when knowledge built from the study of dipolar relaxation phenomena in model resin formulations is transferred to the monitoring of commercial thermosets.

ACKNOWLEDGMENTS

The work reported here was supported by an EPSRC grant GR/R94329 and by EC GROWTH project 'CONDICOMP' (G1RD-2001-03010)

NOMENCLATURE

The symbols are given in alphabetical order

Symbol	Description
c	Adjustable parameter for adaptive mutation
C_{dip}	Dipolar Capacitance
C_{ind}	Induced Capacitance
f	frequency
F	Fitness function
$F_{critical}$	Fitness value above which the genetic algorithm terminates
G	Number of generations
G_{max}	Number of maximum generation
n	Constant Phase Element exponent
N	Number of solution vectors
N_e	Number of solution vectors passing directly to the next generation
N_r	Number of solution vectors passing through crossover and mutation
par	Parameter values
par_{exp}	Expected parameter values

p_e	Exchange probability
p_m	Mutation probability
P_{no}	Number of parameters
q	Number of frequencies in a sweep
R_{dip}	Dipolar resistance
R_{el}	Constant Phase Element parameter
R_{ion}	Ionic resistance
S	Objective function
t	Time
w	Weight factor
Z	Complex impedance
Z'	Real impedance
Z''	Imaginary impedance
λ	Tikhonov regularization parameter
ω	Angular frequency
τ_{dip}	Dipolar relaxation time
Z_{CPE}	Complex impedance of the Constant Phase Element (CPE)

REFERENCES

1. P. Hedvig, *Dielectric Spectroscopy of Polymers*, Adam Hilger Ltd, Bristol, 1977
2. S. D. Senturia, N. F. Sheppard, Dielectric analysis of thermoset cure. *Adv. Polym. Sci.*, 80, 1 (1986)
3. G. M. Maistros, C. B. Bucknall, Modeling the dielectric behavior of epoxy resin blends during curing, *Pol. Eng. Sci.*, 34, 1517 (1994)
4. G. Levita, A. Livi, P. A. Rolla, C. Culicchi, Dielectric monitoring of epoxy Cure, *J. Polym. Sci. Part B: Polym. Phys.*, 34, 2731 (1996)
5. D. Abraham, R. McIlhagger, Glass fibre epoxy composite cure monitoring using parallel plate dielectric analysis in comparison with thermal and mechanical testing techniques, *Composites Part A*, 29A, 811 (1998)
6. P. Bartolomeo, J. F. Chailan, J. L. Vernet, On the use of WLF equation to study curing by dielectric spectroscopy, *Polymer*, 42, 4385 (2001)
7. J. P. Eloundou, Dipolar relaxations on an epoxy – amine system, *Eur. Polym. J.*, 38, 431 (2002)

8. J.-P. Pascault, H. Sautereau, J. Verdu, R. J. J. Williams, *Thermosetting Polymers*, Marcel Dekker Inc., 2002
9. J. Mijovic, F. Bellucci, Impedance spectroscopy of reacting polymers, *Trends Polym. Sci.*, 4, 74 (1995)
10. J. Mijovic, C. F. W. Yee, Use of complex impedance to monitor the progress of reactions in epoxy/amine model systems, *Macromolecules*, 27, 7287 (1994)
11. L. Nicolais, J. Mijovic, F. Bellucci, Impedance spectroscopy of reactive polymers. Correlations with chemorheology during network formation, *J. Electrochem. Soc.*, 142, 1176 (1995)
12. W. Zurawsky, L. Nicolais, I. Mondragon, B. Fitz, J. Mijovic, F. Bellucci, I. Abrahams, Impedance spectroscopy of reactive polymers. 3. Correlations between dielectric, spectroscopic and rheological properties during cure of a trifunctional epoxy resin, *J. Polym. Sci. Pol. Phys.*, 34, 379 (1996)
13. T. Monetta, L. Nicodemo, J. Mijovic, F. Bellucci, V. Maio, Impedance spectroscopy of reactive polymers. 4. An improved experimental procedure for measurement of effective resistivity, *J. Polym. Sci. Pol. Phys.*, 34, 1277 (1996)
14. I. Abrahams, J. Mijovic, F. Bellucci, Impedance spectroscopy of reactive polymers. 5. Impedance as a measure of chemical and physical changes in glass formers, *J. Polym. Sci. Pol. Phys.*, 36, 641 (1998)
15. G. Gallone, G. Levita, J. Mijovic, S. Andjelic, P. A. Rolla, Anomalous trends in conductivity during epoxy – amine reactions, *Polymer*, 39, 2095 (1998)
16. A. A. Skordos, I. K. Partridge, Impedance cure and flow monitoring in the processing of advanced composites, *7th International Conference on the Manufacture of Advanced Composites (ICMAC)*, IoM, Belfast, September 27^{th} – 28^{th}, 2001
17. J. R. Macdonald, *Impedance Spectroscopy. Emphasizing solid materials and systems*, John Wiley & Sons, New York, 1987
18. J. R. Macdonald, Analysis of impedance and admittance data for solids and liquids, *J. Electrochem. Soc.*, 124, 1022 (1977)
19. J. R. Macdonald, Exact and approximate nonlinear least – squares inversion of dielectric relaxation spectra, *J. Chem. Phys.*, 102, 6241 (1995)
20. J. R. Macdonald, Comparison and application of two methods for the least squares analysis of immittance data, *Solid State Ionics*, 58, 97 (1992)
21. J. R. Macdonald, Accurate fitting of immittance spectroscopy frequency-response data using the stretched exponential model, *J. Non-Cryst. Solids*, 212, 95 (1997)
22. J. R. Macdonald, On relaxation-spectrum estimation for decades of data: accuracy and sampling-localization considerations, *Inverse Probl.*, 16, 1561 (2000)
23. R. de L. Kronig, On the theory of dispersion of X – Rays, *J. Opt. Soc. Am.*, 12, 547 (1926)
24. H. A. Kramers, Die dispersion und absorption von Röntgengebeit, *Physik. Z.*, 30, 522 (1929)
25. A. Tarantola, *Inverse Problem Theory*, Elsevier, 1987
26. J. R. Dygas, M. W. Breiter, Variance of errors and elimination of outliers in the least squares analysis of impedance spectra, *Electrochim. Acta*, 44, 4163 (1999)
27. G. H. Golub, P. C. Hansen, D. P. O'Leary, Tikhonov regularization and total least squares, *SIAM J. Matrix Anal. Appl.*, 21, 185 (2000)
28. J. Winterhalter, D. G. Ebling, D. Maier, J. Honerkamp, An improved analysis of admittance data for high resistivity materials by a nonlinear regularization method, *J. Appl. Phys.*, 82, 5488 (1997)
29. J. Winterhalter, D. G. Ebling, D. Maier, J. Honerkamp, Analysis of admittance data: Comparison of a parametric and a nonparametric method, *J. Comput. Phys.*, 153, 139 (1999)

30. LEVM v7.11, http://www.solartronanalytical.com/downloads/software.html , last accessed in 19/03/2004.
31. D. W. Marquardt, An algorithm for least squares estimation of nonlinear parameters, *SIAM J Appl. Math.*, 11, 431 (1963)
32. M. Mitchell, *An introduction to genetic algorithms*, MIT Press, 1998
33. T. J. VanderNoot, I. Abrahams, The use of genetic algorithms in the non-linear regression of immitance data, *J. Electroanal. Chem.*, 448, 17 (1998)
34. M. Yang, X. Zhang, X. Li, X. Wu, A hybrid genetic algorithm for the fitting of models to electrochemical impedance data, *J. Electroanal. Chem.*, 519, 1 (2002)
35. J. Fournier, G. Williams, C. Duch, C., G. A. Aldridge, Changes in molecular dynamics during bulk polymerization of an epoxide-amine system as studied by dielectric relaxation spectroscopy, *Macromolecules*, 29, 7097 (1996)
36. S. Montserrat, F. Roman, P. Colomer, Vitrification and dielectric relaxation during the isothermal curing of an epoxy-amine resin, *Polymer*, 44, 101 (2003)